



THE UNIVERSITY *of* EDINBURGH

Edinburgh Research Explorer

Effect of pH and pressure on uranium removal from drinking water using NF/RO membranes

Citation for published version:

Schulte-Herbruggen, H, Correia Semiao, A, Chaurand, P & Graham, M 2016, 'Effect of pH and pressure on uranium removal from drinking water using NF/RO membranes', *Environmental Science and Technology*, vol. 50, no. 11, pp. 5817–5824. <https://doi.org/10.1021/acs.est.5b05930>

Digital Object Identifier (DOI):

[10.1021/acs.est.5b05930](https://doi.org/10.1021/acs.est.5b05930)

Link:

[Link to publication record in Edinburgh Research Explorer](#)

Document Version:

Peer reviewed version

Published In:

Environmental Science and Technology

General rights

Copyright for the publications made accessible via the Edinburgh Research Explorer is retained by the author(s) and / or other copyright owners and it is a condition of accessing these publications that users recognise and abide by the legal requirements associated with these rights.

Take down policy

The University of Edinburgh has made every reasonable effort to ensure that Edinburgh Research Explorer content complies with UK legislation. If you believe that the public display of this file breaches copyright please contact openaccess@ed.ac.uk providing details, and we will remove access to the work immediately and investigate your claim.



**Effect of pH and pressure on uranium removal from drinking water using
NF/RO membranes.**

Helfrid M.A. Schulte-Herbrüggen^{a*}, Andrea J.C. Semião^a, Perrine Chaurand^b,
Margaret C. Graham^c

^aSchool of Engineering, The University of Edinburgh, Edinburgh, UK

^bAix-Marseille Université, CEREGE, Aix en Provence, France

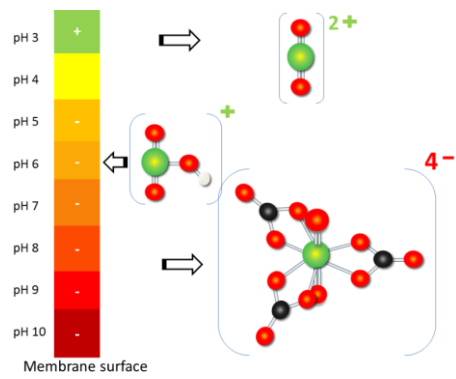
^cSchool of GeoSciences, The University of Edinburgh, Edinburgh, UK

**Current Address:* KTH Royal Institute of Technology, Department for Sustainable
Development, Environmental Science and Engineering (SEED), Teknikringen 76, SE-
100 44 Stockholm, Sweden; *Tel:* +46(0)761624665; *E-mail:* hschulte@kth.se

17 ABSTRACT ART

18

19



20 **Abstract.** Groundwater is becoming an increasingly important drinking water source.
21 However, the use of groundwater for potable purposes can lead to chronic human
22 exposure to geogenic contaminants, *e.g.* uranium. Nanofiltration (NF) and reverse
23 osmosis (RO) processes are used for drinking water purification, and it is important to
24 understand how contaminants interact with membranes since accumulation of
25 contaminants to the membrane surface can lead to fouling, performance decline and
26 possible breakthrough of contaminants. During the current study laboratory
27 experiments were conducted using NF (TFC-SR2) and RO (BW30) membranes to
28 establish the behaviour of uranium across pH (3-10) and pressure (5-15 bar) ranges.
29 The results showed that important determinants of uranium-membrane sorption
30 interactions were (i) the uranium speciation (uranium species valence and size in
31 relation to membrane surface charge and pore size) and (ii) concentration polarisation,
32 depending on the pH values. The results show that it is important to monitor sorption
33 of uranium to membranes, which is controlled by pH and concentration polarisation,
34 and, if necessary, adjust those parameters controlling uranium sorption.

35

36 **Key words:** sorption, concentration polarisation, nanofiltration, reverse osmosis,
37 speciation, uranium

38

39

40

41 **Introduction.** Groundwater is an increasingly important source of drinking water,¹
42 especially for developing nations in *e.g.* Africa² but also in European countries, where
43 20-100% of drinking water is sourced from groundwater.³ As a consequence of
44 hydrological and geochemical processes uranium is naturally present in groundwater
45 at concentrations from below detection to hundreds of $\mu\text{g L}^{-1}$.⁴⁻⁶ Indirect release of
46 uranium into water may also occur through *e.g.* phosphate ore processing, phosphate
47 fertilizer use, gold and tin-mining.⁷⁻¹⁰ Uranium is above all chemically toxic, and
48 although chronic exposure to uranium is not well understood,¹¹⁻¹⁴ studies have
49 identified kidney, bone, liver, heart and brain as potential targets following exposure
50 through ingestion of uranium-containing water.^{11,15-18} The maximum acceptable
51 concentrations (MAC) for uranium vary between public authorities, *e.g.* Canada uses
52 an interim MAC of $20 \mu\text{g L}^{-1}$, whilst the US has adopted the same limit as the WHO
53 provisional drinking water limit of $30 \mu\text{g L}^{-1}$.¹⁹ However, concentrations as low as 2
54 $\mu\text{g/L}$ may be hazardous for infants.²⁰ Membrane technology such as nanofiltration
55 (NF) and reverse osmosis (RO) are frequently used for drinking water purification²¹⁻²⁴
56 since they efficiently remove a wide range of contaminants, including uranium.²⁵
57 Membrane technology is also being considered for application in remote sites due to
58 the modular and flexible configuration and, if coupled with renewable energy, their
59 independence from intermittent or absent energy supplies.²⁶⁻²⁸ The performance of a
60 membrane system using ultrafiltration, NF or RO membranes, coupled with a
61 renewable energy supply was tested in the field. The results showed that although the
62 system performed well in terms of producing permeate with low concentrations of
63 most analytes *e.g.* Ca^{2+} , Mg^{2+} , Mn^{2+} , SO_4^{2-} , Na^+ and Cl^- , the behaviour of uranium in
64 the system differed from that of most other inorganic species found in the water.

Moreover, uranium strongly interacted with the membranes.²⁹ It was deduced that this was largely due to the complex chemical behaviour of uranium, since its speciation varies widely depending on physico-chemical parameters such as available inorganic or organic ligands and pH of the water.^{29–32} For instance, the presence of calcium affects uranium speciation and is likely to affect uranium interaction with the membranes.²⁹ A variety of processes can be responsible for the observed uranium uptake, including precipitation of uranium to the membrane, physi-sorption (such as hydrogen bonding or electrostatic attraction) or chemi-sorption resulting in bond formation between uranium and membrane functional groups. Before the exact mechanisms are determined, the more general terms “sorption” or “uranium-membrane interaction” will be used in this paper. To establish the processes involved in the interaction of uranium with the membrane, controlled laboratory experiments are needed, isolating one factor at a time: individual membranes, solution composition, pH and pressure ranges. The present study focused on uranium in the absence of other major ions, *e.g.* calcium, in order to determine the membrane interactions due to uranium alone. Although there have been studies investigating uranium retention using NF and RO^{33–36} none have investigated the specific interactions between membranes and uranium during the water purification process. Therefore, the aims of this study were to determine (i) the effect of pH and speciation on uranium-membrane interactions by NF and RO membranes; (ii) the effect of membrane pore size and (iii) the effect of pressure on the uranium-membrane interactions.

88 **Materials and Methods.** The behaviour of uranium was investigated using an
89 experimental feed solution containing 0.5 mg L⁻¹ uranium (uranyl nitrate, TAAB,
90 UK), background electrolyte and buffer (20 mM NaCl and 1 mM NaHCO₃, Fisher
91 Scientific, UK). The uranium concentration chosen is comparable to concentrations
92 found naturally.^{4,29,37,38} MilliQ water was used to prepare all solutions (Elga Purelab
93 Ultra, High Wycombe, UK). The pH of the experimental solution was adjusted (1 M
94 HNO₃, VWR Aristar, or 1 M NaOH, Fisher Scientific) according to the conditions to
95 be tested (described later), prior to adding the solution to the stainless steel cross-flow
96 system (MMS, Switzerland). Two membranes with different molecular-weight cut-off
97 (MWCO) values but of similar materials (polyamide active layer on a polysulphone
98 support layer) were selected: TRC-SR2, a NF membrane (Koch Membrane systems,
99 USA) and BW30, a RO membrane (Dow Filmtec). Cross-flow experiments were
100 carried out with and without applied pressure to investigate the effects of pressure on
101 uranium-membrane interactions. Two types of cross-flow experiments were
102 conducted: 1) across the pH range 3-10 (in units of one, with one pH value per
103 experiment) but with *no* applied pressure and 2) at two selected pH values (pH 6 and
104 8.5), across the pressure range 5-15 bar (in steps of 2.5 bar, one pressure and pH value
105 per experiment).

106

107 **Filtration set-up and procedure.** New rectangular membrane coupons (membrane
108 area of 0.0046 m²) were cut for each experiment from a membrane sheet. The
109 coupons were washed and soaked in MilliQ water at 4°C overnight, washed again,
110 before being mounted in the stainless steel cross-flow system, operated in total
111 recirculation mode. Membranes were compacted using MilliQ water at 25 bar prior to

112 experiments and a solution sample was collected as a quality check. A detailed
 113 description of the experimental set-up is given in the supporting information (SI) and
 114 a schematic is published in Semião and Schäfer.³⁹ The system was drained and
 115 experimental solution added (feed volume of 2 L). The flow-rate was set to 0.6 L min⁻¹
 116 and, for *pressure experiments*, pressure was applied at this point. Temperature,
 117 pressure, feed flow, feed and permeate pH and conductivity were monitored
 118 throughout the experiments which lasted up to seven hours. Feed and permeate
 119 samples were regularly collected. The pH value of the feed solution was adjusted (1
 120 M HNO₃, VWR Aristar, or 1 M NaOH) during experiments to maintain the pH value
 121 within ± 0.2 . The pH value of permeate samples deviated from that of the feed with
 122 up to a value of ± 0.5 .

123

124 The mass of uranium sorbed by the membrane (mg U m⁻² of membrane) was simply
 125 calculated as the mass uptake of uranium by the membrane divided by the membrane
 126 area. To report the mass sorbed as percentage uptake, the uranium mass sorbed by the
 127 membrane was calculated in relation to the initial mass of uranium available in the
 128 feed (*i.e.* 1 mg U):

129

$$Uptake(\%) = \frac{V_{b0}C_{b0} - V_{bf}C_{bf} - \sum_{i=0}^{i=n} V_S C_{si}}{V_{b0}C_{b0}} \times 100 \quad \text{Eq. 1}$$

133

134 where, V = volume (L), C = uranium concentration (mg L^{-1}), s = permeate or feed
135 sample taken, b = bulk (or feed), f = final, 0 = initial and n indicates the number of
136 samples collected during the experiment.

137

138 Following completion of each experiment and the removal of the membrane, the
139 system was thoroughly washed using dilute HNO_3 (2%, v/v Analar, VWR) followed
140 by consecutive washes with MilliQ water. For quality control purposes a sample was
141 collected of the final system washes and analysed for uranium content (below
142 detection in washes).

143

144 **Chemical analysis and quality control.** The uranium concentrations in the feed
145 samples was determined by Inductively Coupled Plasma – Optical Emission
146 Spectroscopy (ICP-OES, Optima 5300 DV, Perkin Elmer, USA) whilst those in the
147 permeate samples were determined by Inductively Coupled Plasma – Mass
148 Spectrometry (ICP-MS, Agilent 7500ce). Calibration standards were prepared using a
149 uranium stock solution ($1000 \text{ mg L}^{-1} \text{ U}$, Merck) and dilute HNO_3 (2% v/v, Aristar,
150 VWR International, UK). For both ICP-OES and ICP-MS analysis, check standards
151 and blank samples (2% v/v HNO_3) were inserted after every 5-10 samples during the
152 run. The accuracy of the calibration was asserted for both techniques by analyzing a
153 standard reference solution (ICP Multi Element Standards Solution VI, Certipur). The
154 average value obtained for the standard reference material during ICP-OES analysis
155 was $0.978 \pm 0.140 \text{ mg L}^{-1}$ (expected: $1.0 \pm 0.05 \text{ mg L}^{-1}$). The average value for the
156 ICP-MS analysis was $0.979 \pm 0.59 \text{ } \mu\text{g L}^{-1}$ (expected: $1.0 \pm 0.05 \text{ } \mu\text{g L}^{-1}$).

157

Micro-X-ray Fluorescence spectroscopy. The penetration of uranium into membranes was explored for selected experiments using micro-X-ray Fluorescence spectroscopy (μ -XRF, XGT-7000 microscope from Horiba Jobin Yvon). Cross-sections of the dry membranes were cut using scissors and placed between paperboard support for analysis in a line over multiple points (1000s/point) along the membrane cross-section with an incident X-ray beam size of 10 μ m (Rh target, accelerating voltage of 50 kV, current 1 mA). More detailed information on this method is provided in the Supporting Information.

Speciation modeling. The modeling of the uranium and other ions present in the aqueous solution was carried out across the pH range 3-10 using visual Minteq 2.53 (KTH, Stockholm, Sweden), as described in Rossiter et al.²⁹

Membrane characterization. NF and RO membranes have been shown by other studies to have different surface chemistries. The BW30 membrane consists of a fully aromatic polyamide active layer coated with an aliphatic layer rich in alcoholic groups, whilst other membranes have a fully or semi aromatic polyamide active layer with no coating.⁴⁰ As these different functional groups may affect membrane surface charge⁴¹ and hence potentially, the interaction with different uranium species, the membrane zeta potential was measured in background electrolyte solution (1 mM NaHCO₃ and 20 mM NaCl) using an electro-kinetic analyzer (EKA, Anton Paar, Austria). MWCO and pore-size was determined experimentally using a range of neutral organic molecules (dioxane, dextrose (Fisher, UK), xylose (Acros Organics, UK) and polyethylene glycol of different molecular weight (400, 600 and 1000 g mol⁻¹

¹, Fisher, UK)) at a concentration of 25 mg carbon L⁻¹ applied to the same membrane sample, following methods described in Hilal et al. and Nghiem et al.^{42,43} For the determination of pore radius, film theory was used⁴⁴ and a correlation was used to estimate the mass transfer coefficient of UO₂²⁺.^{45,46} Organic carbon concentrations were measured in non-purgeable organic carbon mode using a TOC Analyser (Shimadzu TOC-VCPH, UK) with an ASI autosampler and high-sensitivity catalyst. Salt flux was calculated using conductivity measurements. Average permeability and standard deviation of the membrane coupons was calculated using the stabilized flux measurements during compaction.

Results and Discussion.

Membrane characterisation. The zeta potential measurements showed that the net charge of TFC-SR2 and BW30 were similar to each other and varied with pH: the overall charge was positive at pH 3, the iso-electric points for TFC-SR2 and BW30 were at pH 4.25 and pH 4.19 (Table 1), respectively, after which the magnitude of the negative charge increased with increasing pH value. The nominal MWCO (90% retention), permeability measurements and pore radius calculation showed that TFC-SR2 has a more open structure compared with BW30 (Table 1).

Uranium sorption to NF and RO membrane across the pH range 3-10. The objective of these experiments was to determine the influence of pH on the extent of uranium sorption by the membrane without the application of pressure. The results for uranium sorption by the membrane are shown in Figure 1 together with the dominant uranium species across the pH range. Sorption increased from < 5.5% at pH 3 for both

membranes, to a maximum of 31% for BW30 and 50% for TFC-SR2 at pH 6. Thereafter sorption decreased to < 10% at pH 10 for both membranes. Notably, the sorption was similar for both membranes at the pH extremes, whereas, although following the same pattern, the sorption was at least 20% lower for BW30 at peak sorption than for TFC-SR2.

The results of these experiments confirm the observations by Rossiter et al.²⁹ that there is a strong interaction between uranium and NF/RO membranes, especially at pH values 5-7. The speciation modelling showed that the dominant uranium species vary greatly with pH and the valence of the uranium species also changed from being positive at acidic pH (pH 3-6), to either neutral or carrying single negative charge under near-neutral conditions to highly negative at alkaline pH (pH 8-10). Since the overall membrane charge also varies with pH, going from weakly positive (pH 2-4) to highly negative at pH values above pH 5, charge interactions are likely to play an important role in uranium sorption. Electrostatic repulsion can explain the low interaction between uranium and the membranes at pH 3-4 and pH 8-10, where uranium species and membrane carry the same charge. Electrostatic attraction is a likely contributor to the greater sorption of uranium to the membrane at pH 5 and 6, which was 49% for the TFC-SR2 and varied from 25 to 31% for the BW30 membrane. Charge interactions between uranium species and NF/RO membranes hence govern uranium sorption to the membranes.

The uranium species also vary in molecular weight (Table 2), and hence size exclusion might contribute to the difference in sorption for both membranes studied.

230 At pH 5-6, where high uranium sorption takes place, the MW of the main uranium
231 species (UO_2OH^+ , UO_2^{2+} and UO_2CO_3 , Figure 1) is considerably lower (270-330 g
232 mol^{-1}) than the MWCO of the TFC-SR2 membrane (MWCO: 486 g mol^{-1}). The size
233 difference between the membrane MWCO and the uranium species, allied to charge
234 attraction between the negatively charged membrane and the positively charged or
235 neutral uranium species, suggests ease in penetrating the TFC-SR2 membrane⁴⁷ in the
236 absence of pressure and with access to the active and support layers for sorption.
237 Charge attraction will also occur between the uranium species and the BW30
238 membrane, as both TFC-SR2 and BW30 membranes have similar negative surface
239 charge.⁴⁸ However, the BW30 membrane has a MWCO of 88 g mol^{-1} , hence based on
240 size exclusion, a much lower uranium penetration into the membrane active layer and
241 support layer would be expected. In fact, the sorption by TFC-SR2 reached
242 equilibrium more slowly (generally 30-60 minutes longer) than for BW30, which
243 would be consistent with slower diffusion of uranium, followed by sorption into the
244 porous active and support layer structure. The higher sorption onto the TFC-SR2
245 membrane as opposed to the BW30 membrane could hence be caused by a higher
246 surface area available for the uranium species to sorb onto the membrane.

247 To provide further evidence for the penetration of uranium into the TFC-SR2
248 membrane, μ -XRF analysis was performed on four selected membrane samples after
249 experiments at pH 6 and pH 8.5 for both BW30 and TFC-SR2. These pH values were
250 selected in order to investigate a point of high sorption of uranium at pH 6 and one of
251 lower uranium sorption at pH 8.5. The μ -XRF analysis showed significant differences
252 with regards to uranium distribution for both membranes studied (Figure 2). As the
253 spatial resolution of this method is relatively low (the incident X-ray beam size is 10

254 μm and penetrates through the sample so the lateral resolution is very low *i.e.* mm
255 range), the exact location of uranium cannot be conclusively determined, *i.e.* whether
256 uranium is present in the active layer, support layer or both, since the NF/RO
257 membrane active layers have a thickness of around 200 nm.⁴⁹ Neither the thickness of
258 the active layer nor that of the membrane can be accurately determined with this
259 method as the method picks up the sulfur signal of the polysulphone support layer but
260 not the signal corresponding to the polyester support layer. However, the sulfur
261 signals indicate the presence of the polysulfone support layer, whereas the calcium
262 signals indicate the *approximate* boundaries of the membrane since the calcium
263 signals originate from the mounting material (see Supporting Information). The XRF
264 analysis presented in Figure 2 a confirms that uranium entered into the more open
265 membrane structure of the TFC-SR2 at pH 6, as the uranium peak for this membrane
266 overlapped with the sulfur peak. In contrast, no uranium could be detected for the
267 BW30 membrane (Figure 2 c), showing low or no penetration into this membrane.
268 Size exclusion hence plays an important role in uranium sorption. At pH 8.5, albeit
269 lower compared to pH 6 due to charge repulsion, uranium penetration and internal
270 sorption occurred for the TFC-SR2 membrane (Figure 1 and Figure 2 b). This
271 occurred independently of conditions of charge repulsion between the negatively
272 charged membrane and the negatively charged uranium species, showing the effect of
273 membrane pore size and hence size exclusion in uranium penetration and sorption into
274 the membrane structure. Uranium sorption onto the more opened TFC-SR2 membrane
275 is hence not only governed by charge interactions but also by access to internal
276 surface area governed by membrane pore size. In contrast, no uranium could be
277 detected for the BW30 membrane for pH 8.5, as can be seen in Figure 2 d, showing

that any sorption observed in Figure 1 by this membrane was not likely to occur deep inside the membrane structure but mainly on the surface: uranium sorption for the dense RO membrane is hence governed by charge interactions. The lower penetration into BW30 compared to TFC-SR2 hence indicates that membrane pore size acts as a limiting factor to sorption of uranium by the membranes. Pore size has similarly been determined as an important factor in membrane sorption of hormones.⁵⁰

Uranium sorption by membrane at pressures 5-15 bar. The previous section demonstrated the higher penetration of uranium species into the membrane of greater porosity (TFC-SR2), across the pH range and irrespective of uranium species present. The objective of these experiments was to investigate the effect of pressure on the uranium sorption to the membranes. Pressure is likely to enhance the permeation of solutes inside the membrane and hence facilitate access to the internal membrane surface area, where sorption may occur. It may also lead to a higher concentration of uranium at the membrane surface (through concentration polarisation) and, as a consequence, precipitation might occur. To investigate this, a pressure range of 5-15 bar was selected based on the typical range for spiral wound membranes (3-20 bar)⁵¹ and manufacturer recommendations.^{52,53} Again, pH values 6 and 8.5 were selected.

The resulting membrane sorption of uranium as a function of pressure is presented in Figure 3. The sorption varied significantly between membrane types and also between pH values and thus uranium species present. For TFC-SR2 at pH 6, a constant sorption of $50 \pm 5\%$ of uranium (equivalent to a range of 109-125 mg U m⁻² of the membrane surface) was observed across the pressure range (5-12.5 bar) (Figure 3a);

only at 15 bar was there a significant increase in uranium sorption to 69%. The sorption for the same membrane but at pH 8.5 was different: sorption *increased with pressure*, from < 20% at 5 bar up to 61% at 12.5 and 15 bar (Figure 3b). Conversely, for BW30 the sorption of uranium by the membrane remained unaffected by pressure at both pH 6 and pH 8.5 (Figure 3c and d). The results show that irrespectively of pressure and pH, uranium sorption is higher in TRC-SR2 than in BW30. TFC-SR2 also gave lower retention for uranium, across the pressure range of 5-15 bar: $90\% \pm 6\%$ at pH 6, $94\% \pm 5\%$ at pH 8.5 while for BW30 uranium retention was $99.7\% \pm 0.3\%$ for both pH values and across the entire pressure range. The results are consistent with the larger pore size of TFC-SR2 compared to BW30 which is related with permeability. The permeability of the two membranes were compared using the pure water flux before and after completed experiments, and the permeate flux during experiments (Figure 4). Pure water flux for BW30 was approximately half of that for TFC-SR2 at the same pressure, reflecting the difference in permeability between the two membranes. As expected, BW30 experienced a flux decline during the uranium experiments, consistent with effects of concentration polarisation and osmotic pressure difference between the feed and permeate side.⁵⁴ Once the pure water flux was again measured after the uranium experiments, it was restored to its original value. By contrast, the flux of TFC-SR2 unexpectedly increased with the addition of experimental solution (and also with addition of salt solution not containing uranium; results not included) and remained high even when the experimental solution was drained and pure water was filtered. Although unusual, a similar effect has been reported by several studies.^{55–57} Nilsson et al. linked the flux increase to pore expansion caused by salt ions reducing the strength of the membrane cross-links.⁵⁷

Such pore expansion within the TFC-SR2 membrane would further enhance the penetration of uranium into the membrane.

328

Furthermore, concentration polarisation, which increases with increasing permeability, is likely to affect the filtration, leading to an accumulation of solutes and consequently higher concentration adjacent to the membrane surface. Taking concentration polarisation into account, the solute concentration at the membrane surface was calculated using Equation 2,⁴⁴

334

$$\frac{C_m - C_p}{C_b - C_p} = \exp\left(\frac{J_v}{k}\right) \quad \text{Eq. 2}$$

337

where C_m = concentration at membrane surface (mg L^{-1}), C_p = concentration in permeate (mg L^{-1}), C_b = concentration in bulk solution (mg L^{-1}), J_v = permeate flux (m s^{-1}) and k = the mass transfer coefficient (m s^{-1}). Whereas C_p , C_b and J_v are determined experimentally, k had to be calculated using correlations relevant to the experimental conditions (slit channel and laminar flow). For the experimental conditions of the system used, the Sherwood number can be related to the Reynolds and Schmidt number⁵⁸ as described in Equation 3:

345

$$Sh = 1.85 \times Re^{0.33} Sc^{0.33} (d_h / L)^{0.33} \quad \text{Eq. 3}$$

347

348 where Re = the Reynolds number, Sc = the Schmidt number, dh = channel hydraulic
349 diameter, L = the length of the membrane cell. The Reynolds, Schmidt and Sherwood
350 number were calculated as described in Semião et al.³⁷

351

352 The extent of concentration polarisation experienced by a membrane can be reported
353 as the concentration polarisation modulus, giving the ratio of initial concentration at
354 the membrane surface (C_m) to that in the bulk solution (C_b) at the start of the
355 experiment. The concentration polarisation modulus for each pressure experiment are
356 displayed together with the uranium uptake in Figure 3. During filtration with BW30,
357 uranium uptake (around 30 and 20% for pH 6 and 8.5, respectively) for both pH
358 values remained unaffected by pressure and concentration polarisation (Figure 3c and
359 d). Due to its high permeability the TFC-SR2 membrane was more affected than
360 BW30 by concentration polarisation. There were some important differences between
361 the results for TFC-SR2 at the two pH values. At pH 8.5, uranium sorption to the
362 membrane clearly followed the polarisation modulus trend. This trend was similar to a
363 previous study with hormones and a NF270 membrane, where higher polarisation
364 modulus resulted in higher concentration at the membrane surface translating into a
365 higher adsorption.³⁷ In contrast, at pH 6 the uranium uptake to the TFC-SR2
366 membrane remained constant despite pressure and concentration polarisation increase,
367 with the exception of the highest pressure point. It appears that concentration
368 polarisation does not affect the interaction between the uranium species and
369 membrane at pH 6, suggesting that variations in uranium concentration only have a
370 small effect on the amount of uranium sorbed by the membranes. To confirm this, an
371 adsorption isotherm for uranium at pH 6 was plotted (Figure S2). Using linear fit of

the sorption isotherm, the uranium sorption, based on the concentration at the membrane surface C_m of 0.62-1.03 mg L⁻¹ for pressures 5 to 15, was estimated to around 107-123 mg U m⁻² of membrane surface, i.e. a sorption of 50% to 57% based on mass balance, showing that pressure and hence concentration polarisation had an insignificant effect on uranium sorption at pH 6. Precipitation as an uptake mechanism could be excluded, as even at high concentration polarisation the uranium concentration at the membrane surface was calculated to be a maximum of 1.03 mg L⁻¹ and still remained below maximum solubility of uranium, thus confirming sorption to be the main mechanism governing uranium-membrane interactions.

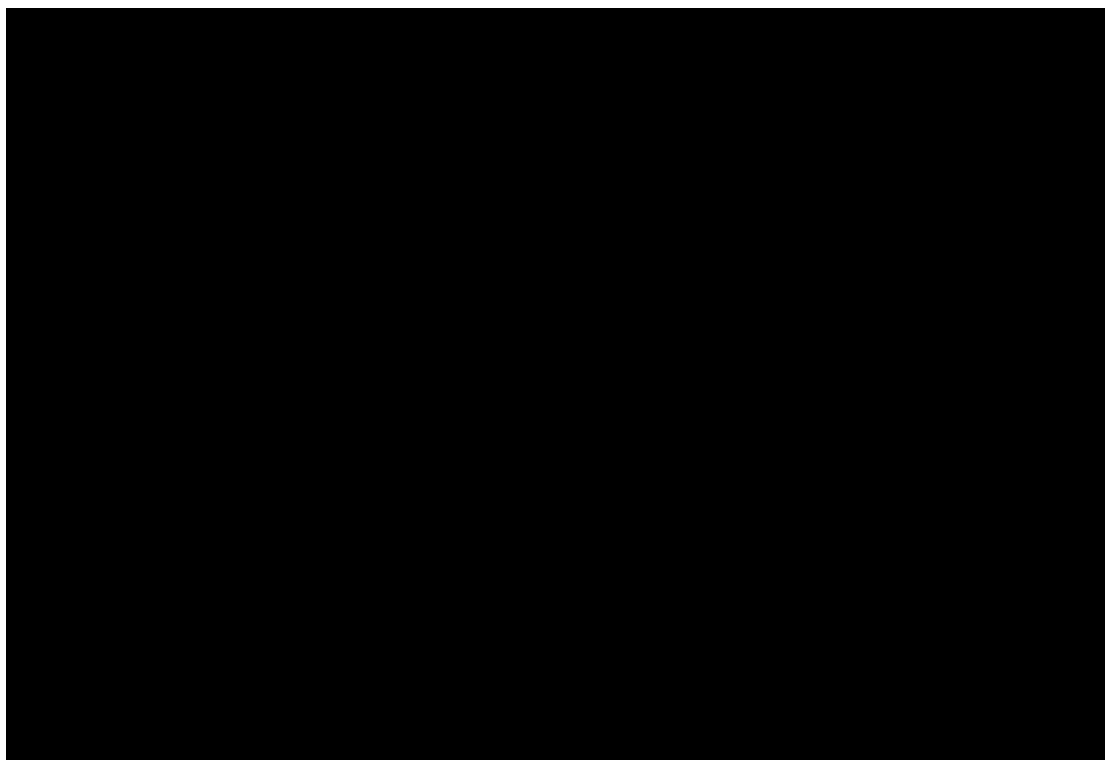
This study confirmed that the uranium-membrane interactions were highly speciation and pH dependent, with affinity determined by the charge of both membrane and uranium species (*e.g.* UO_2OH^+ or $\text{UO}_2(\text{CO}_3)_3^{4-}$) as well as species size relative to membrane pore size. Pore size and subsequent permeability of the membranes governed uranium sorption, where TFC-SR2 was subject to higher uranium sorption than BW30 under all experimental conditions. Concentration polarisation affected only one of the uranium species, $\text{UO}_2(\text{CO}_3)_3^{4-}$, a species which generally tends to display low sorption and high mobility,^{59,60} but its sorption to TFC-SR2 increased with increasing pressure. UO_2OH^+ , whose sorption to TFC-SR2 was initially higher, remained largely unaffected by concentration polarisation. This study has provided a first insight into the nature of the interactions of uranium with NF and RO membranes and the clear effects of pH and charge interactions, membrane pore size and concentration polarisation on uranium sorption. Uranium sorption might be further affected by the presence of different functional groups on the membrane active layer.

Tang et al,⁶¹ for example, showed that some RO membranes possess a surface layer coating rich in -COH groups in addition to the aromatic or semi-aromatic polyamide active layer. Hence, future work focused on a more in-depth analysis to determine the chemical nature and spatial distribution of the uranium sorption to the membranes, as well as the effect of hardness on the removal of uranium by NF and RO membranes is needed.

The results are of significance in the wider membrane application context since it illustrates the importance of taking sorption of contaminants into account. The retention *observed* in experimental and applied water treatment settings may not be the actual or real retention, and the long-term consequences of sorption to the membranes remains unknown. One possible consequence is the risk of uranium desorption from the membrane into the permeate line during operation, especially at acidic pH values, which could pose a health risk to water consumers. There is great variability in membrane life-time and performance from location to location and contaminant sorption (not necessarily picked up since it may not cause obvious fouling and consequent flux decline) may be one of the determining factors.

417 FIGURES

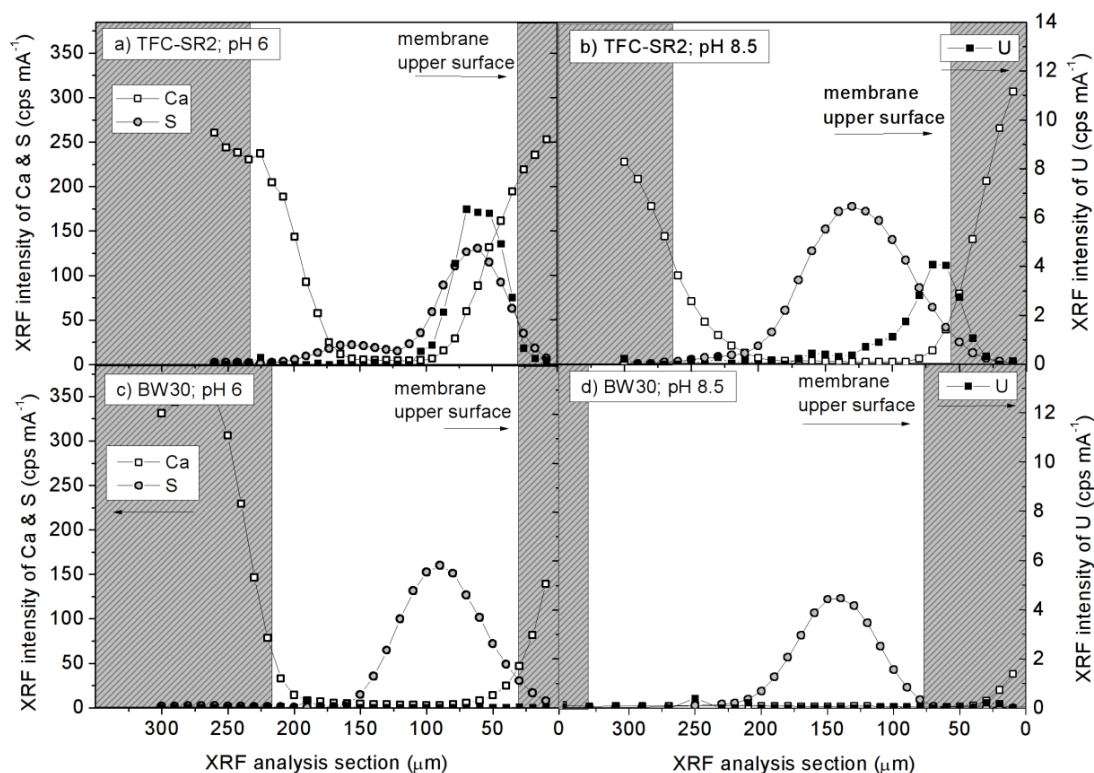
418



419

420 Figure 1. Uranium speciation (lines) and uranium uptake or sorption (columns)
421 by membranes TFC-SR2 and BW30 across the pH range 3-10. Experimental
422 solution: 0.5 mg L⁻¹ uranium, 20 mM NaCl and 1 mM NaHCO₃. Experimental
423 conditions: flow-rate = 0.6 L min⁻¹, temperature = 24°C, no applied pressure.
424 The variation in uptake was within ± 4% for repeated experiments for TFC-
425 SR2 and ± 1% for BW30.

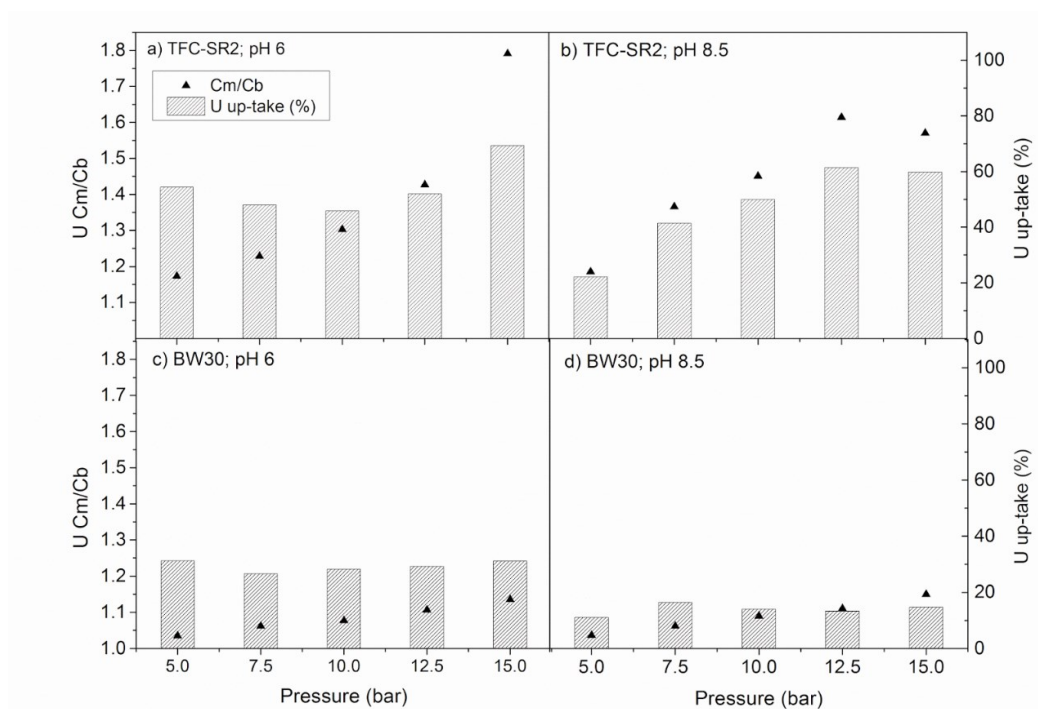
426



427

428 Figure 2. Cross-sections of TFC-SR2 and BW30 showing the elemental
 429 distribution of U, S and Ca for experiments performed without pressure for
 430 TFC-SR2 at pH 6 (a) and pH 8.5 (b) and BW30 at pH 6 (c) and pH 8.5 (d)
 431 determined by μ -XRF. The *approximate* top and bottom edge of the
 432 membrane is indicated by the shaded area based on the detection of the
 433 calcium mounting material. Note the different intensity scales for Ca and S
 434 compared to U.

435



436

437 Figure 3. The percentage uptake (sorption) of uranium (columns) during the
 438 experiments is shown on the right y-axis, while the calculated polarisation
 439 modulus (Cm/Cb) for uranium is indicated by points and displayed on the left
 440 y-axis. Repeatability of U uptake for selected experiments was within $\pm 4\%$ for
 441 TFC-SR2 and $\pm 1\%$ for BW30.

442

443

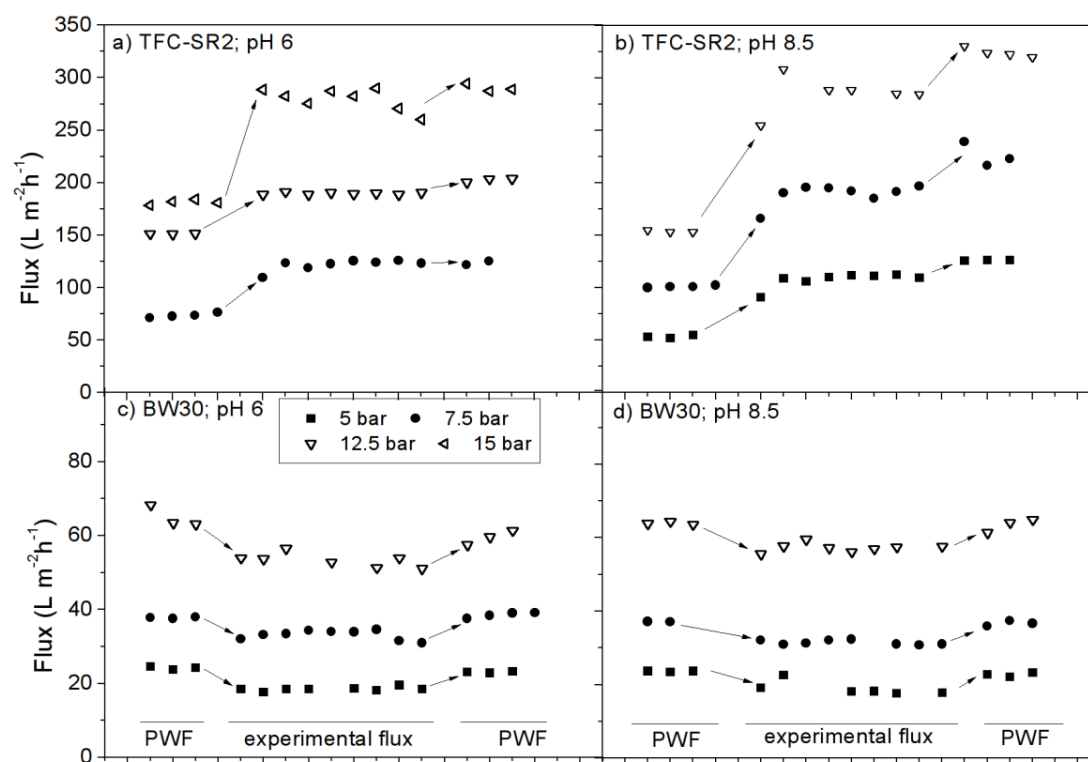


Figure 4. Pure water flux (PWF) before and after selected pressure experiments, and permeate flux during pressure experiments (5-15 bar) for TFC-SR2 and BW30 at pH 6 and 8.5. Permeability variability for TFC-SR2 was $\pm 13\%$ and BW30 was $\pm 3\%$ based on pure water flux experiments. Variability of permeate flux during experiments was within $\pm 10\%$ for TFC-SR2 and $\pm 2\%$ for the BW30. Please note different flux scales for TFC-SR2 and BW30.

TABLES

Table 1. Membrane characteristics

Parameter	TFC-SR2	BW30
Iso-electric point/pH	4.25	4.19
Nominal MWCO/g mol ⁻¹	486 ^a	88
Pore radius/nm	0.52 \pm 0.03	0.32 \pm 0.01 ^{b,43}
Permeability/L m ⁻² h ⁻¹ bar ⁻¹	10.97 \pm 1.51	4.84 \pm 0.15

^aAbsolute MWCO (100% retention) for TFC-SR2 was determined as 1033 g mol⁻¹.

^bNote that RO membranes are considered to have dense, non-porous structures and so “pore-radius” for BW30 was determined only as a comparison with the more open structure of TFC-SR2.

Table 2. Main uranium species present for pH range 3-10^a

pH value	Uranium species	Molecular weight (g mol ⁻¹)
3-4	UO ₂ ²⁺	270
5-6	UO ₂ OH ⁺	287

6-7	UO_2CO_3	330
7	$(\text{UO}_2)_2\text{CO}_3(\text{OH})_3^-$	651
8	$\text{UO}_2(\text{CO}_3)_2^{2-}$	390
8-10	$\text{UO}_2(\text{CO}_3)_3^{4-}$	450

^aNote that each pH value may contain a mixture of several species.

ASSOCIATED CONTENT

Supporting information. Details of experimental set-up and filtration procedure, ICP-OES, ICP-MS and XRF analysis, salt retention and isotherm experiment. This material is available free of charge via the internet at <http://pubs.acs.org>.

AUTHOR INFORMATION

Corresponding Author

*Tel +46 (0)87906291

E-mail: hschulte@kth.se

Present Addresses

*Department for Sustainable Development, Environmental Science and Engineering (SEED), KTH Royal Institute of Technology, Teknikringen 76 1 tr, SE-100 44 Stockholm, Sweden.

Author Contributions

The manuscript was written through contributions of all authors. All authors have given approval to the final version of the manuscript.

Funding Sources

ESRC-EPSRC PhD scholarship, FFWG for additional living allowance and EPSRC Doctoral Prize Fellowship for H. Schulte-Herbrüggen.

ACKNOWLEDGMENT

Acknowledgements. The authors are grateful to the following organisations and individuals: The School of Engineering (University of Edinburgh, UoE) for funding cross-flow equipment, Koch Membrane Systems and Filmtec Corporation for NF and RO membrane sheets, Dr Annalisa De-Munari (UoE), Dr Alexander Bismarck and Dr Kingsley Ho (Imperial College, UK) for zeta potential measurements, Steven Gourlay (UoE) for cross-flow system design, Dr Alan Simm (UoE) for LabVIEW set up, Dr Lorna Eades (UoE) for assistance with ICP-MS analysis. Prof Andrea Schäfer (UoE) is thanked for facilitating the work and Prof Viatcheslav Freger (Technion, Israel) and the anonymous reviewers are thanked for constructive suggestions to improve the work.

References.

- (1) Wada, Y.; van Beek, L. P. H.; van Kempen, C. M.; Reckman, J. W. T. M.; Vasak, S.; Bierkens, M. F. P. Global depletion of groundwater resources. *Geophys. Res. Lett.* **2010**, *37* (20), L20402.
- (2) MacDonald, A. M.; Bonsor, H. C.; Dochartaigh, B. É. Ó.; Taylor, R. G. Quantitative maps of groundwater resources in Africa. *Environ. Res. Lett.* **2012**, *7* (2), 24009.

- 508 (3) Estrela, T.; Marcuello, C.; Iglesias, A. *Water resources problems in Southern*
509 *Europe*; 1996.
- 510 (4) Nriagu, J.; Nam, D.-H.; Ayanwola, T. A.; Dinh, H.; Erdenechimeg, E.; Ochir,
511 C.; Bolormaa, T.-A. High levels of uranium in groundwater of Ulaanbaatar,
512 Mongolia. *Sci. Total Environ.* **2012**, *414*, 722–726.
- 513 (5) Norrström, A. C.; Löf, Å. Uranium theoretical speciation for drinking water
514 from private drilled wells in Sweden – Implications for choice of removal
515 method. *Appl. Geochem.* **2014**, *51*, 148–154.
- 516 (6) Vesterbacka, P. Natural radioactivity in drinking water in private wells in
517 Finland. *Radiat. Prot. Dosimetry* **2004**, *113* (2), 223–232.
- 518 (7) Winde, F.; Jacobus van der Walt, I. The significance of groundwater–stream
519 interactions and fluctuating stream chemistry on waterborne uranium
520 contamination of streams—a case study from a gold mining site in South Africa.
521 *J. Hydrol.* **2004**, *287* (1–4), 178–196.
- 522 (8) Arogunjo, A. M.; Höllriegl, V.; Giussani, A.; Leopold, K.; Gerstmann, U.;
523 Veronese, I.; Oeh, U. Uranium and thorium in soils, mineral sands, water and
524 food samples in a tin mining area in Nigeria with elevated activity. *J. Environ.*
525 *Radioact.* **2009**, *100* (3), 232–240.
- 526 (9) Vandenhove, H.; Sweeck, L.; Mallants, D.; Vanmarcke, H.; Aitkulov, A.;
527 Sadyrov, O.; Savosin, M.; Tolongutov, B.; Mirzachev, M.; Clerc, J. J.; et al.
528 Assessment of radiation exposure in the uranium mining and milling area of
529 Mailuu Suu, Kyrgyzstan. *J. Environ. Radioact.* **2006**, *88* (2), 118–139.
- 530 (10) H. Vandenhove. European sites contaminated by residues from the ore-
531 extracting and -processing industries. *Int. Congr. Ser.* **2002**, *1225*, 307–325.
- 532 (11) Craft, E. S.; Abu-Qare, A. W.; Flaherty, M. M.; Garofolo, M. C.; Rincavage, H.
533 L.; Abou-Donia, M. B. Depleted and natural uranium: chemistry and
534 toxicological effects. *J. Toxicol. Environ. Health Part B* **2004**, *7* (4), 297–317.
- 535 (12) Kurttio, P.; Harmoinen, A.; Saha, H.; Salonen, L.; Karpas, Z.; Komulainen, H.;
536 Auvinen, A. Kidney Toxicity of Ingested Uranium From Drinking Water. *Am. J.*
537 *Kidney Dis.* **2006**, *47* (6), 972–982.
- 538 (13) Prat, O.; Vercouter, T.; Ansoborlo, E.; Fichet, P.; Perret, P.; Kurttio, P.; Salonen,
539 L. Uranium speciation in drinking water from drilled wells in southern Finland
540 and its potential links to health effects. *Environ. Sci. Technol.* **2009**, *43* (10),
541 3941–3946.
- 542 (14) Vicente-Vicente, L.; Quiros, Y.; Perez-Barriocanal, F.; Lopez-Novoa, J. M.;
543 Lopez-Hernandez, F. J.; Morales, A. I. Nephrotoxicity of Uranium:
544 Pathophysiological, Diagnostic and Therapeutic Perspectives. *Toxicol. Sci.* **2010**,
545 *118* (2), 324–347.
- 546 (15) Miller, A. C.; Brooks, K.; Smith, J.; Page, N. Effect of the militarily-relevant
547 heavy metals, depleted uranium and heavy metal tungsten-alloy on gene
548 expression in human liver carcinoma cells (HepG2). *Mol. Cell. Biochem.* **2004**,
549 *255* (1–2), 247–256.
- 550 (16) Hogan, A.; Vandam, R.; Markich, S.; Camilleri, C. Chronic toxicity of uranium
551 to a tropical green alga (sp.) in natural waters and the influence of dissolved
552 organic carbon. *Aquat. Toxicol.* **2005**, *75* (4), 343–353.
- 553 (17) Kurttio, P.; Auvinen, A.; Salonen, L.; Saha, H.; Pekkanen, J.; Mäkeläinen, I.;
554 Väisänen, S. B.; Penttilä, I. M.; Komulainen, H. Renal effects of uranium in
555 drinking water. *Environ. Health Perspect.* **2002**, *110* (4), 337.

- 556 (18) Kurttio, P.; Komulainen, H.; Leino, A.; Salonen, L.; Auvinen, A.; Saha, H. Bone
557 as a Possible Target of Chemical Toxicity of Natural Uranium in Drinking
558 Water. *Environ. Health Perspect.* **2004**, *113* (1), 68–72.
- 559 (19) World Health Organization. *Guidelines for drinking-water quality*; World
560 Health Organization: Geneva, 2011.
- 561 (20) Birke, M.; Rauch, U.; Lorenz, H.; Kringel, R. Distribution of uranium in German
562 bottled and tap water. *J. Geochem. Explor.* **2010**, *107* (3), 272–282.
- 563 (21) Cyna, B.; Chagneau, G.; Bablon, G.; Tanghe, N. Two years of nanofiltration at
564 the Méry-sur-Oise plant, France. *Desalination* **2002**, *147* (1–3), 69–75.
- 565 (22) Service, R. F. Desalination Freshens Up. *Science* **2006**, *313* (5790), 1088–1090.
- 566 (23) Al-Amoudi, A.; Lovitt, R. W. Fouling strategies and the cleaning system of NF
567 membranes and factors affecting cleaning efficiency. *J. Membr. Sci.* **2007**, *303*
568 (1–2), 4–28.
- 569 (24) Van der Bruggen, B.; Vandecasteele, C. Removal of pollutants from surface
570 water and groundwater by nanofiltration: overview of possible applications in
571 the drinking water industry. *Environ. Pollut.* **2003**, *122* (3), 435–445.
- 572 (25) Annanmäki, M.; STUK Radiation and Nuclear Safety Authority. *Treatment*
573 *techniques for removing natural radionuclides from drinking water. Final report*
574 *of the TENAWA project*; 2000.
- 575 (26) Thomson, M.; Infield, D. A photovoltaic-powered seawater reverse-osmosis
576 system without batteries. *Desalination* **2003**, *153* (1–3), 1–8.
- 577 (27) Coffey, M. Renewable energy: Filtration and the green energy revolution. *Filtr.*
578 *Sep.* **2008**, *45* (5), 24–27.
- 579 (28) De Munari, A.; Schäfer, A. I. Membrane plants for drinking water provision in
580 remote scottish communities: performance, costs and lessons learnt. In
581 *Membranes in Drinking and Industrial Water*; Trondheim, Norway, 2010.
- 582 (29) Rossiter, H. M. A.; Graham, M. C.; Schäfer, A. I. Impact of speciation on
583 behaviour of uranium in a solar powered membrane system for treatment of
584 brackish groundwater. *Sep. Purif. Technol.* **2010**, *71* (1), 89–96.
- 585 (30) Kantar, C. Heterogeneous processes affecting metal ion transport in the presence
586 of organic ligands: Reactive transport modeling. *Earth-Sci. Rev.* **2007**, *81* (3–4),
587 175–198.
- 588 (31) Semião, A. J. C.; Rossiter, H. M. A.; Schäfer, A. I. Impact of organic matter and
589 speciation on the behaviour of uranium in submerged ultrafiltration. *J. Membr.*
590 *Sci.* **2010**, *348* (1–2), 174–180.
- 591 (32) Langmuir, D. *Aqueous Environmental Geochemistry*; Prentice-Hall, Inc.: Upper
592 Saddle River, New Jersey, 1997.
- 593 (33) Huikuri, P.; Salonen, L.; Raff, O. Removal of natural radionuclides from
594 drinking water by point of entry reverse osmosis. *Desalination* **1998**, *119* (1),
595 235–239.
- 596 (34) Raff, O.; Wilken, R.-D. Removal of dissolved uranium by nanofiltration.
597 *Desalination* **1999**, *122* (2), 147–150.
- 598 (35) Favre-Reguillon, A.; Lebizit, G.; Foos, J.; Guy, A.; Draye, M.; Lemaire, M.
599 Selective Concentration of Uranium from Seawater by Nanofiltration. *Ind. Eng.*
600 *Chem. Res.* **2003**, *42* (23), 5900–5904.
- 601 (36) Favre-Réguillon, A.; Lebizit, G.; Murat, D.; Foos, J.; Mansour, C.; Draye, M.
602 Selective removal of dissolved uranium in drinking water by nanofiltration.
603 *Water Res.* **2008**, *42* (4–5), 1160–1166.

- 604 (37) Orloff, K. G.; Mistry, K.; Charp, P.; Metcalf, S.; Marino, R.; Shelly, T.; Melaro,
605 E.; Donohoe, A. M.; Jones, R. L. Human exposure to uranium in groundwater.
606 *Environ. Res.* **2004**, *94* (3), 319–326.
- 607 (38) Seldén, A. I.; Lundholm, C.; Edlund, B.; Högdahl, C.; Ek, B.-M.; Bergström, B.
608 E.; Ohlson, C.-G. Nephrotoxicity of uranium in drinking water from private
609 drilled wells. *Environ. Res.* **2009**, *109* (4), 486–494.
- 610 (39) Semião, A. J. C.; Schäfer, A. I. Estrogenic micropollutant adsorption dynamics
611 onto nanofiltration membranes. *J. Membr. Sci.* **2011**, *381* (1–2), 132–141.
- 612 (40) Tang, C. Y.; Kwon, Y.-N.; Leckie, J. O. Effect of membrane chemistry and
613 coating layer on physiochemical properties of thin film composite polyamide RO
614 and NF membranes: I. FTIR and XPS characterization of polyamide and coating
615 layer chemistry. *Desalination* **2009**, *242* (1–3), 149–167.
- 616 (41) Tang, C.; Kwon, Y.; Leckie, J. Probing the nano- and micro-scales of reverse
617 osmosis membranes—A comprehensive characterization of physiochemical
618 properties of uncoated and coated membranes by XPS, TEM, ATR-FTIR, and
619 streaming potential measurements. *J. Membr. Sci.* **2007**, *287* (1), 146–156.
- 620 (42) Hilal, N.; Al-Abri, M.; Al-Hinai, H. Characterization and retention of UF
621 membranes using PEG, HS and polyelectrolytes. *Desalination* **2007**, *206* (1–3),
622 568–578.
- 623 (43) Nghiem, L. D.; Schäfer, A. I.; Elimelech, M. Removal of Natural Hormones by
624 Nanofiltration Membranes: Measurement, Modeling, and Mechanisms. *Environ.*
625 *Sci. Technol.* **2004**, *38* (6), 1888–1896.
- 626 (44) Sutzkover, I.; Hasson, D.; Semiat, R. Simple technique for measuring the
627 concentration polarization level in a reverse osmosis system. *Desalination* **2000**,
628 *131* (1), 117–127.
- 629 (45) Gekas, V.; Hallström, B. Mass transfer in the membrane concentration
630 polarization layer under turbulent cross flow: I. Critical literature review and
631 adaptation of existing sherwood correlations to membrane operations. *J. Membr.*
632 *Sci.* **1987**, *30* (2), 153–170.
- 633 (46) van den Berg, G. B.; Rácz, I. G.; Smolders, C. A. Mass transfer coefficients in
634 cross-flow ultrafiltration. *J. Membr. Sci.* **1989**, *47* (1–2), 25–51.
- 635 (47) Borrini, J.; Bernier, G.; Pellet-Rostaing, S.; Favre-Reguillon, A.; Lemaire, M.
636 Separation of lanthanides(III) by inorganic nanofiltration membranes using a
637 water soluble complexing agent. *J. Membr. Sci.* **2010**, *348* (1–2), 41–46.
- 638 (48) Negaresh, E.; Antony, A.; Bassandeh, M.; Richardson, D. E.; Leslie, G.
639 Selective separation of contaminants from paper mill effluent using
640 nanofiltration. *Chem. Eng. Res. Des.* **2012**, *90* (4), 576–583.
- 641 (49) Freger, V. Swelling and Morphology of the Skin Layer of Polyamide Composite
642 Membranes: An Atomic Force Microscopy Study. *Environ. Sci. Technol.* **2004**,
643 *38* (11), 3168–3175.
- 644 (50) Semião, A. J. C.; Schäfer, A. I. Removal of adsorbing estrogenic micropollutants
645 by nanofiltration membranes. Part A—Experimental evidence. *J. Membr. Sci.*
646 **2013**, *431*, 244–256.
- 647 (51) Thorsen, T.; Fløgstad, H. *Nanofiltration in drinking water treatment*; Literature
648 review D5. 3. 4B; Techneau, 2006.
- 649 (52) Dow Filmtec. Dow Filmtec Membranes.
- 650 (53) Koch Membrane Systems. Fluid Systems TFC-SR2 2.5" Element.

- (54) Sablani, S.; Goosen, M.; Al-Belushi, R.; Wilf, M. Concentration polarization in ultrafiltration and reverse osmosis: a critical review. *Desalination* **2001**, *141* (3), 269–289.
- (55) Wang, Y.; Shu, L.; Jegatheesan, V.; Gao, B. Removal and adsorption of diuron through nanofiltration membrane: The effects of ionic environment and operating pressures. *Sep. Purif. Technol.* **2010**, *74* (2), 236–241.
- (56) De Munari, A.; Schäfer, A. I. Impact of speciation on removal of manganese and organic matter by nanofiltration. *J. Water Supply Res. Technol.* **2010**, *59* (2–3), 152.
- (57) Nilsson, M.; Trägårdh, G.; Östergren, K. The influence of sodium chloride on mass transfer in a polyamide nanofiltration membrane at elevated temperatures. *J. Membr. Sci.* **2006**, *280* (1–2), 928–936.
- (58) Schock, G.; Miquel, A. Mass transfer and pressure loss in spiral wound modules. *Desalination* **1987**, *64*, 339–352.
- (59) Wazne, M.; Meng, X.; Korfiatis, G. P.; Christodoulatos, C. Carbonate effects on hexavalent uranium removal from water by nanocrystalline titanium dioxide. *J. Hazard. Mater.* **2006**, *136* (1), 47–52.
- (60) Maher, K.; Bargar, J. R.; Brown, G. E. Environmental Speciation of Actinides. *Inorg. Chem.* **2013**, *52* (7), 3510–3532.
- (61) Tang, C. Y.; Kwon, Y.-N.; Leckie, J. O. Effect of membrane chemistry and coating layer on physiochemical properties of thin film composite polyamide RO and NF membranes. *Desalination* **2009**, *242* (1–3), 168–182.